Research article

GS-KG9 ameliorates diabetic neuropathic pain induced by streptozotocin in rats

Jee Youn Lee [1], Hae Young Choi [1], Chan Sol Park [2], Mi Kyung Pyo [3], Tae Young Yune [1,2,4,**], Go Woon Kim [5], Sung Hyun Chung [5,*]

[1] Age-Related and Brain Diseases Research Center, Kyung Hee University, Seoul, Republic of Korea
[2] KHU-KIST Department of Converging Science and Technology, Kyung Hee University, Seoul, Republic of Korea
[3] International Ginseng and Herb Research Institute, Geumsan, Republic of Korea
[4] Department of Biochemistry and Molecular Biology, School of Medicine, Kyung Hee University, Seoul, Republic of Korea
[5] Department of Pharmacology and Clinical Pharmacy, College of Pharmacy, Kyung Hee University, Seoul, Republic of Korea

ARTICLE INFO

ABSTRACT

Background: Diabetic neuropathy is one of the most devastating ailments of the peripheral nervous system. Neuropathic pain develops in ∼30% of diabetics. Here, we examined the suppressive effect of GS-KG9 on neuropathic pain induced by streptozotocin (STZ).
Methods: Hyperglycemia was induced by intraperitoneal injection of STZ. Rats showing blood glucose level > 250 mg/dL were divided into five groups, and treatment groups received oral saline containing GS-KG9 (50 mg/kg, 150 mg/kg, or 300 mg/kg) twice daily for 4 wk. The effects of GS-KG9 on pain behavior, microglia activation in the lumbar spinal cord and ventral posterolateral (VPL) nucleus of the thalamus, and c-Fos expression in the dorsal horn of the lumbar spinal cord were examined.
Results: The development of neuropathic pain began at Day 5 and peaked at Week 4 after STZ injection. Mechanical and thermal pains were both significantly attenuated in GS-KG9-treated groups from 10 d after STZ injection as compared to those in the STZ control. GS-KG9 also repressed microglia activation in L4 dorsal horn and VPL region of the thalamus. In addition, increase in c-Fos-positive cells within L4 dorsal horn lamina I and II of the STZ control group was markedly alleviated by GS-KG9.
Conclusion: These results suggest that GS-KG9 effectively relieves STZ-induced neuropathic pain by inhibiting microglial activation in the spinal cord dorsal horn and VPL region of the thalamus.
© 2017 The Korean Society of Ginseng, Published by Elsevier Korea LLC. This is an open access article under the CC BY-NC-ND license (http://creativecommons.org/licenses/by-nc-nd/4.0/).

1. Introduction

Diabetes mellitus is a metabolic disorder with semeiotic symptoms such as polyuria, polyphagia, and polydipsia along with low-grade inflammation [1,2]. Neuropathic pain, one of the devastating complications of diabetes mellitus, is a neurological illness exhibiting hyperalgesia and allodynia. Since pathophysiological mechanisms of neuropathic pain are complex and multifactorial, current treatments are far from remission and often worsen a glucose homeostasis.

Inflammatory responses play a pivotal role in the development of neuropathic pain [3,4]. Ginseng extract and total saponin have anti-inflammatory effects in lipopolysaccharide- and/or β-amyloid-stimulated microglial cells [5]. It is also reported that ginsenoside Rb1 attenuates acute inflammatory pain by inhibiting neuronal extracellular signal-regulated kinase (ERK) phosphorylation via regulation of the Nrf2 and nuclear factor (NF)-κB pathways [6]. However, the effect of ginseng extracts on diabetic neuropathic pain has not yet been examined.

Here, we examined whether GS-KG9, an air-dried and ethanol extracted white ginseng, had an analgesic effect on STZ-induced neuropathic pain. We also investigated the mitigated effect of GS-KG9 on microglial activation in L4—L5 dorsal horn and ventral posterolateral (VPL) nucleus of the thalamus as an underlying

mechanism. Additionally, the expression of c-Fos in dorsal horn of L4–L5 spinal cord was examined and compared to that in STZ controls.

2. Materials and methods

2.1. GS-KG9 preparation and HPLC analysis

Korean ginseng (*Panax ginseng* Meyer, 4 yr old) was purchased from the local market in Geumsan, Korea. A mixture of white ginseng and white ginseng tail (6:4, w/w) dried at 55°C for 5 d in an air dryer was extracted with 70% ethanol three times at 40°C. The white ginseng extract was filtered and concentrated *in vacuo*, and named as GS-KG9. Ten milligrams of GS-KG9 was dissolved in 1 mL methanol and filtered through a 0.45-µm-membrane filter after extraction with ultrasonic waves for 30 min, and analyzed by HPLC. The HPLC system used was Waters 1525 (Waters Corporation, Milford, MA, USA) with a photodiode array detector. A Waters Xbridge C18 column (250mm × 4.6mm, 5µm) was used for analysis of ginsenosides. The detection wavelength, flow rate, injection volume, and column oven temperature were set at 203 nm, 1.0 mL/min, 20 µL, and 40°C, respectively. The mobile phase consisted of purified water with 0.03% trifluoroacetic acid (A) and acetonitrile (B) using the following gradient program: 0 min 18% B, 42 min 24% B, 46 min 29% B, 79 min 40% B, 115 min 65% B, 135 min 85% B, and 160 min 18% B.

2.2. Animals and drug administration

Male Sprague–Dawley rats (6 wk old, 190–210 g; Samtako, Osan-Shi, Korea) were raised in an animal room with uniform humidity (60 ± 10%) and temperature (23 ± 1°C) under a 12-h light/dark cycle with free access to water and food. Hyperglycemia was induced by intraperitoneal injection of STZ (60 mg/kg; Sigma-Aldrich, St. Louis, MO, USA) and control animals received the same volume of saline. Four days after STZ injection, hyperglycemia and hypoinsulinemia were confirmed by using an Accu-Chek Compact Plus glucose meter (Roche Diagnostics, Meylan, France) and a rat insulin ELISA kit (Millipore, Billerica, MA, USA), respectively. Blood glucose levels were increased to 366.2 ± 23.1 mg/dL from 118.4 ± 3.8 mg/dL, and serum insulin levels were reduced to 0.9 ± 0.3 ng/mL from 3.6 ± 0.4 ng/mL after STZ injection, suggesting that the chemically induced diabetic model was successfully developed. Animals showing blood glucose level > 250 mg/dL were selected and randomly divided into five groups including normal, STZ control, and three treatment groups. GS-KG9 (50 mg/kg, 150 mg/kg, or 300 mg/kg) was dissolved in saline and administered orally twice daily for 4 wk. All experiments were done according to the protocol approved by the Institutional Animal Care and Use Committee (IACUC) of Kyung Hee University, Seoul, Korea (permission number: KHUASP(SE)-16-069).

2.3. Physiological markers of diabetes

Fasting blood glucose concentration (mg/dL) was measured in the tail vein once weekly using an Accu-Chek Compact Plus glucose meter (Roche Diagnostics) and serum insulin level was determined at Day 4 after STZ injection using a rat insulin ELISA kit. Body weight and drinking water (mL/d) and food (g/d) consumption were determined every day during the 4-wk experimental period.

2.4. Behavioral tests for pain

2.4.1. Mechanical pain
Mechanical pain was examined by the paw withdrawal threshold (PWT) in reaction to probing with a series of calibrated von Frey filaments (3.92–147.0 mN equivalent to 0.4–15.0 g; Stoelting, Wood Dale, IL, USA). The 50% withdrawal threshold was determined by using an up–down method [7]. Animals were placed under transparent plastic boxes (28 cm × 10 cm × 10 cm) on a metal mesh floor, and left alone for 20 min before the sensory test began. Stimuli were applied for 3–4 s to each hind paw while the filament was bent and presented at intervals of several seconds. A swift hind paw withdrawal to von Frey filament application was regarded as a positive response.

2.4.2. Thermal pain
Heat sensitivity was assessed according to the method developed by Hargreaves et al. [8] to determine the paw withdrawal latency (PWL) in reaction to radiant heat (Model 390; IITC Life Science Inc., Woodland Hills, CA, USA). Animals were acclimated to the apparatus equipped with six Perspex boxes on an elevated glass table. A heat source under the glass table was applied to the center of the plantar surface. The heat intensity was set to produce PWL of about 10 s, and cut-off time was set at 20 s to prevent tissue damage. Three times of heat stimuli were given for each paw at an interval of 5–10 min, and the mean PWL was taken.

2.5. Tissue preparation and immunohistochemistry

At 4 wk after GS-KG9 administration, animals were anesthetized with 500 mg/kg chloral hydrate and perfused with 0.1M phosphate-buffered saline (pH 7.4) and then with 4% paraformaldehyde. Brain and spinal cord L4–L5 segments were removed, postfixed by immersion in the same fixative for 5 h, and placed in 30% sucrose. The tissues were embedded in optimal cutting temperature compound for cryosectioning, as previously described [9], and transverse sections were cut at 20µm or 30µm using a cryostat (CM1850; Leica, Wetzlar, Germany). For the molecular study, animals were perfused with 0.1M phosphate-buffered saline and spinal cord segments (L4–L5) were removed and frozen at −80°C until use. Tissue sections were embedded in 3% hydrogen peroxide for 10 min at room temperature to suppress endogenous peroxidase activity. After washing with Tris-buffered saline with 0.1% Triton X-100 (TBS-T), the sections were immersed in 5% normal serum (Vector Laboratories Inc., Burlingame, CA, USA) in TBS-T for 1 h at room temperature to prevent nonspecific binding, and then incubated with a rabbit anti-c-Fos (1:100; Millipore) and OX-42 (1:200; Millipore) overnight at 4°C. Some sections stained for c-Fos were double-labeled using neuronal cell marker, NeuN (1:100; Millipore). For double labeling, fluorescein-isothiocyanate- or Cy3-conjugated secondary antibodies (Jackson Immuno Research, West Grove, PA, USA) were used. Nuclei were also labeled with 4′,6-diamidino-2-phenylindole (Molecular Probes, Eugene, OR, USA). For control experiments, reaction to the substrate was absent whenever a primary antibody was omitted or replaced by a nonimmune, control antibody. Immunofluorescent sections were mounted with Vectashield mounting medium (Vector Laboratories). Fluorescence-labeled signals were detected by a fluorescence microscope (BX51; Olympus, Tokyo, Japan), and image capture and measurement of signal colocalization was performed with MetaMorph software (Molecular Devices, Sunnyvale, CA, USA).

2.6. Quantitative analysis

Immunohistochemistry images were captured using a microscope along with the Cool SNAP camera (Roper Scientific, Sarasota, FL, USA). A person who did not know the treatment history of the animals performed quantitative analysis blindly. To determine the microglia activation in L4–L5 spinal cord, the percentage of field

analysis was used to provide a quantitative estimate of changes in the activation status of microglia. Resting and activating microglia were classified and counted based on a previous report [10]. Using immunostaining with OX-42, resting microglia were displayed as small compact somata bearing long, thin, and ramified processes. By contrast, activating microglia exhibited marked cellular hypertrophy and retraction of processes, such that the process length was less than the diameter of the soma compartment. Cells were collected when the nucleus was visible within the plane of section and cells exhibited distinctly delineated borders. OX-42-positive cells were counted for a predefined area of superficial layer of spinal cord (lamina I and II). For quantification of c-Fos-positive cells in L4−L5 spinal cord dorsal horn, three transverse sections of L4−L5 segment in each animal were collected and c-Fos-positive cells in the superficial layer (lamina I and II) were manually counted from each field and averaged. For quantitative analysis of microglia activation in the VPL nucleus of the thalamus, OX-42 intensity in three transverse sections of each animal was analyzed using Metamorph software (Molecular Devices, Sunnyvale, CA, USA).

2.7. Statistical analysis

All data are presented as mean ± standard deviation. Comparisons between STZ control and GS-KG9-treated groups were made by unpaired Student t test. Multiple comparisons between groups were performed by one-way analysis of variance. Tukey's multiple comparison was used for *post hoc* analysis. Statistical significance was indicated by $p < 0.05$. SPSS version 15.0 (SPSS Inc., Chicago, IL, USA) was used for statistical analyses.

3. Results

3.1. HPLC profile of GS-KG9

Dried GS-KG9 had 116.3 mg/g crude saponin extract and ginsenosides such as Rg1, Re, Rf, Rb1, malonyl-Rb1, Rc, malonyl-Rc, Rb2, malonyl-Rb2, Rb3, Rd, and malonyl-Rd (Fig. 1). Malonyl Rb1, Rb2, Rc, and Rd representing Peaks 5, 7, 10, and 12 were sharply separated and even higher than those of corresponding well-known ginsenosides (Peaks 4, 6, 8, and 11).

3.2. STZ-induced hyperglycemia is suppressed by GS-KG9

Blood glucose levels were significantly increased in STZ-treated rats at 7 d, 14 d, 21 d, and 28 d when compared to those in normal rats (Fig. 2A). Parallel to hyperglycemia, STZ caused marked weight loss (Fig. 2B), polyphagia (Fig. 2C), and polydipsia (Fig. 2D). GS-KG9,

however, markedly decreased blood glucose level in STZ-treated rats compared to the vehicle-treated group over the experimental period in a dose-dependent manner (Fig. 2A and E). The body weight of the GS-KG9-treated group was higher than that of the STZ control group, although there was no significant significance (Fig. 2B). However, there were no significant differences in food and water consumption between the GS-KG9-treated and STZ control groups (Fig. 2C and D).

3.3. GS-KG9 inhibits STZ-induced mechanical and thermal pain

To determine the analgesic effect of GS-KG9 in the STZ-induced hyperglycemic model, we first examined whether chronic neuropathic pain was developed by STZ. PWT and PWL to mechanical and thermal stimuli, respectively, were reduced significantly after STZ treatment in a time-dependent manner (Fig. 3A and C). At Day 35 after STZ injection, hyperglycemic rats displayed mechanical and thermal pain (STZ group: PWT; 2.7 ± 0.9 g, PWL; 6.2 ± 0.8 s, vs. Normal group: PWT; 15.0 ± 0.0 g, PWL; 12.9 ± 0.7 s; Fig. 3A and C). Next, we investigated the analgesic effects of GS-KG9 on STZ-induced neuropathic pain at Day 28 after GS-KG9 administration. GS-KG9 (150 mg/kg and 300 mg/kg) significantly alleviated STZ-induced mechanical pain (PWT, STZ + 150 mg/kg GS-KG9: 10.2 ± 2.3 g, STZ + 300 mg/kg GS-KG9: 11.5 ± 1.8 g vs. STZ: 2.9 ± 1.6 g) and thermal pain (PWL, STZ + 150 mg/kg GS-KG9: 9.5 ± 0.9 s, STZ + 300 mg/kg GS-KG9: 10.1 ± 1.3 s vs. STZ: 5.6 ± 1.4 s) when compared to those in vehicle-treated group (Fig. 3B and D). However, a low dose (50 mg/kg) of GS-KG9 seems not to be enough for relieving pain. These results indicate that GS-KG9 has significant analgesic effects on STZ-induced mechanical and thermal pain.

3.4. GS-KG9 inhibits microglial activation in L4−L5 spinal cord

Microglial activation in the spinal cord dorsal horn is evident in several models of neuropathic pain including diabetic neuropathy [11−16]. Under physiological conditions, microglia display a small soma bearing thin-branched processes. When activated, cell bodies become hypertrophic, thickened, and retracted (Fig. 4D). To examine the inhibitory effect of GS-KG9 on microglial activation in L4−L5 spinal cords, immunohistochemistry using an antibody against OX-42 was performed at 28 d after GS-KG9 administration. Microglia were counted in the lamina I−II layers of spinal cord dorsal horn, which are the sites of unmyelinated Aδ and C fibers responsible for nociceptive signal processing, and large myelinated Aβ fibers terminated (Fig. 4A−C, dotted box). Morphology of OX-42-positive cells in normal rats displayed a small soma bearing thin-branched or ramified processes, indicating a resting state (Fig. 4A). After STZ injection,
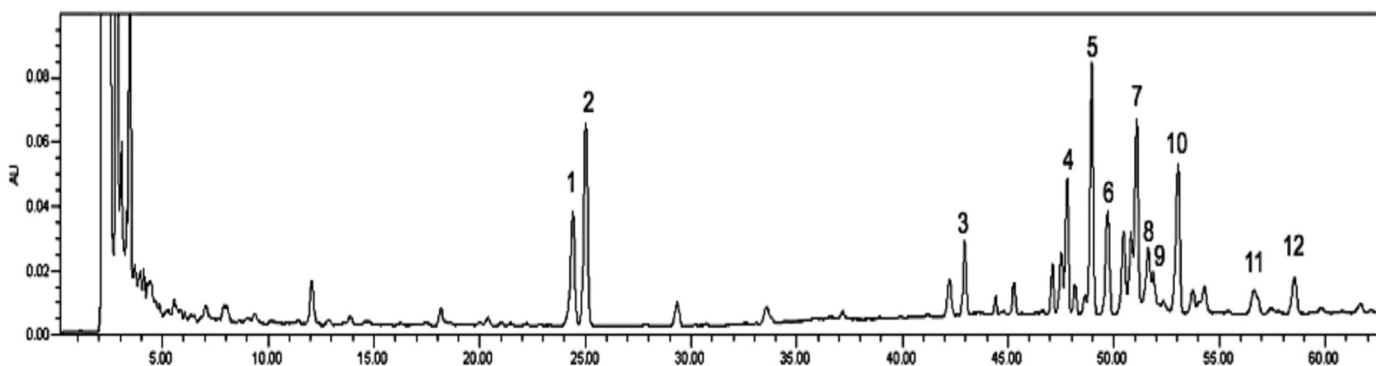
Fig. 1. HPLC profile of GS-KG9, which is an air-dried and ethanol extracted white ginseng. Number above each peak indicates as follows: 1, Rg1; 2, Re; 3, Rf; 4, Rb1; 5, m-Rb1; 6, Rc; 7, m-Rc; 8, Rb2; 9, Rb3; 10, m-Rb2; 11, Rd; and 12, m-Rd.
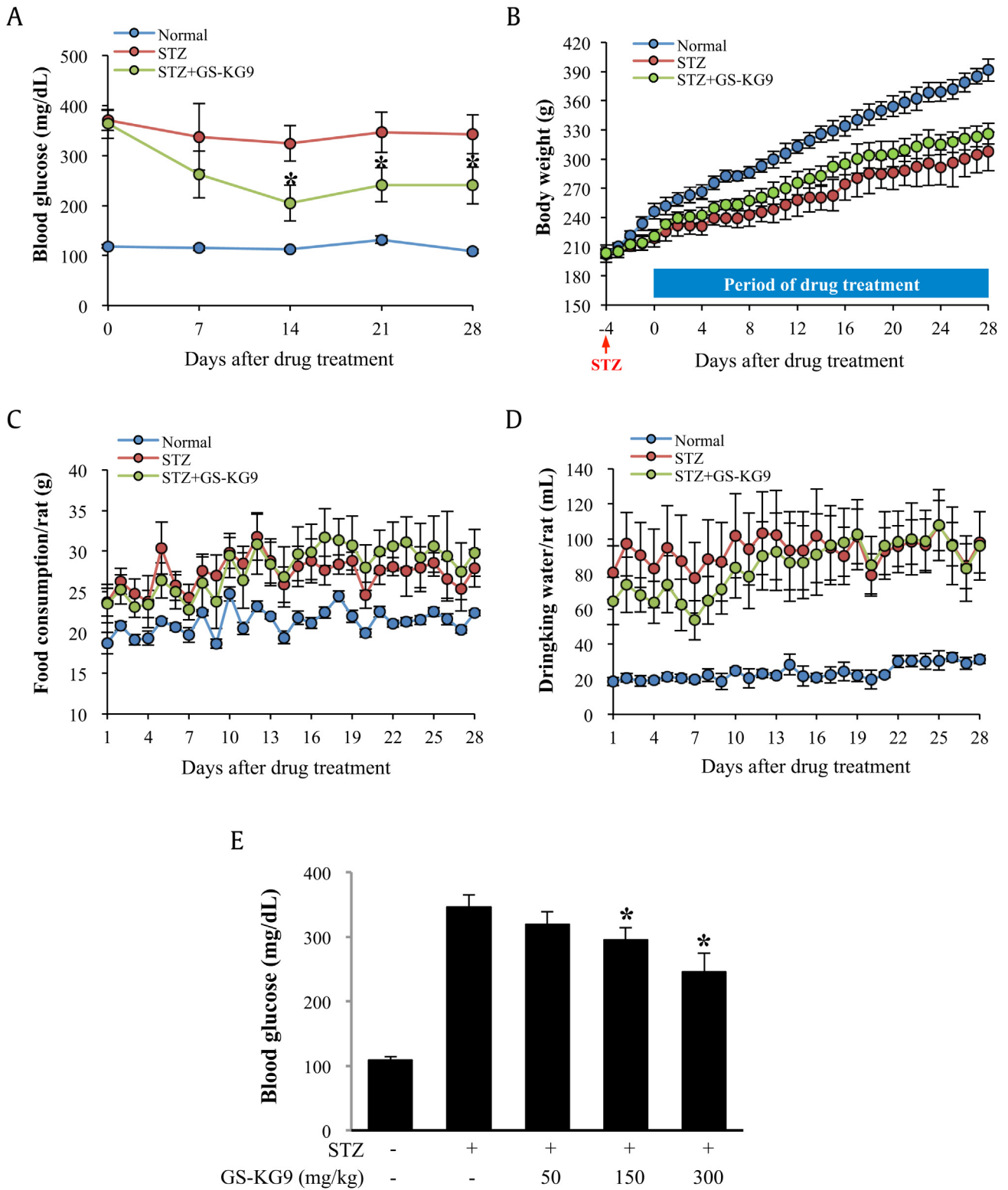
Fig. 2. Effects of GS-KG9 on blood glucose level, body weight, and drinking water and food consumptions in STZ-induced hyperglycemic rats. Hyperglycemia was induced in male Sprague−Dawley rats by injecting STZ (60 mg/kg, intraperitoneally). At Day 5 after STZ injection, rats were randomly divided into vehicle- and GS-KG9-treated groups. GS-KG9 (300 mg/kg) was administered orally twice daily for 4 wk. During 4 wk after drug administration, blood glucose level (A), body weight (B), food consumption (C), and drinking water consumption (D) were measured. Effects of three different doses of GS-KG9 on blood glucose level are presented in E. Data are expressed as the mean ± standard deviation (n = 10 rats/group). *p < 0.05 versus STZ control. STZ, streptozotocin.
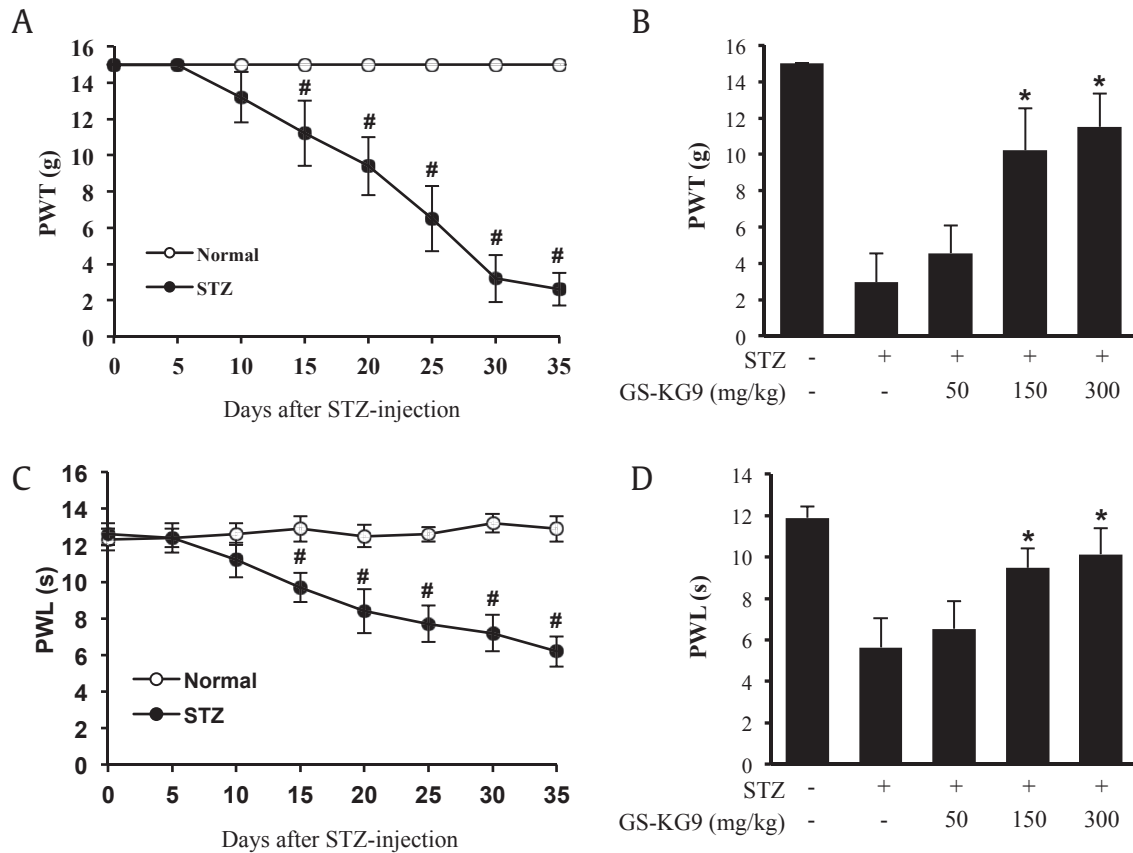
Fig. 3. GS-KG9 inhibits STZ-induced neuropathic pain. (A,C) Pain responses to mechanical (PWT) and heat stimuli (PWL) after STZ injection. Rats with STZ-induced neuropathic pain were treated with GS-KG9 (50 mg/kg, 150 mg/kg, or 300 mg/kg) twice daily for 4 wk (*n* = 10 rats/group). At 28 d after GS-KG9 administration, GS-KG9 significantly increased mechanical PWT (B) and thermal PWL (D) in a dose-dependent manner compared to those in vehicle-treated rats. Data are expressed as the mean ± standard deviation. #*p* < 0.05 versus Normal, **p < 0.05 versus STZ control. PWL, pain withdrawal latency; PWT, pain withdrawal threshold; STZ, streptozotocin.

OX-42-positive cells showed marked cell body hypertrophy and retraction of cytoplasmic processes (Fig. 4B). Quantitative analysis revealed a higher proportion of activated microglia (86.8 ± 7.3%) in the STZ-treated group than in the normal controls (7.9 ± 1.2%; Fig. 4D). In STZ-induced hyperglycemic rats, GS-KG9 significantly decreased the number of activated microglia when compared to those in the STZ control group (STZ + GS-KG9: 41.4 ± 5.8% vs. 86.8 ± 8.2%; Fig. 4C and D). These results indicate that microglia were activated in L4−L5 spinal dorsal horn of STZ-induced hyperglycemic rats, and GS-KG9 significantly attenuated microglia activation.

3.5. GS-KG9 inhibits c-Fos expression in L4−L5 spinal cord

We determined the expression of c-Fos, a marker of neuronal activation in the lumbar spinal cord, at 28 d after GS-KG9 administration. c-Fos expression patterns in the spinal cord are known to be correlated with the type, intensity, and duration of nociceptive stimuli. Immunocytochemistry showed that the number of c-Fos immunoreactive cells was significantly increased in the superficial layer (lamina I, II) of L4−L5 spinal cord dorsal horn in STZ-induced hyperglycemic rats when compared to those in normal rats (Fig. 5A). However, the number of c-Fos-positive cells in GS-KG9-treated groups was reduced when compared to that in the STZ control group (Fig. 5A). Parallel to morphological observation, quantitative analysis revealed that GS-KG9 significantly decreased the number of c-Fos-positive cells in spinal cord dorsal horn by 43.5% compared to the STZ control group (STZ + GS-KG9: 47.5 ± 8.6 vs. STZ: 84.2 ± 8.9 cells; Fig. 5C). In addition, double labeling showed that most of the c-Fos-positive cells were colocalized with NeuN, suggesting that c-Fos was expressed mainly in neurons (Fig. 5B).

3.6. GS-KG9 inhibits microglia activation in the VPL of the thalamus

Besides the spinal cord, functional changes in pain mediating areas in the brain have been closely engaged in diabetic neuropathic pain. Among these areas, marked morphological changes in the thalamus, cortex, and rostroventromedial medulla have been documented in patients with diabetic neuropathic pain and experimental models [17,18]. The VPL of the thalamus is a major receiving area of nociceptive stimuli through the spinal cord [19]. Projection neurons reach the thalamus via the spinothalamic tract; a major ascending nociceptive pathway, and these neurons exhibit increased spontaneous activity, enlargement of the receptive field, and augmented responses to mechanical and thermal stimuli in diabetic rats. The hyperexcitability of spinothalamic tract neurons may account for hypersensitivity to external stimuli and spontaneous pain [20,21]. Recent studies have shown that thalamic glial alterations occur in various pain models such as central, peripheral, and inflammatory pain [12,22−24]. To determine the effect of GS-KG9 on microglial activation in the VPL, we performed immunostaining with an antibody against OX-42 using brain tissues prepared at 28 d after GS-KG9 administration. Resting microglia in normal rats displayed small, compact soma with long, thin, and ramified processes (Fig. 6). In addition, OX-42 immunoreactivity was increased and the activated microglia exhibited marked cellular hypertrophy and retraction of processes in STZ-induced
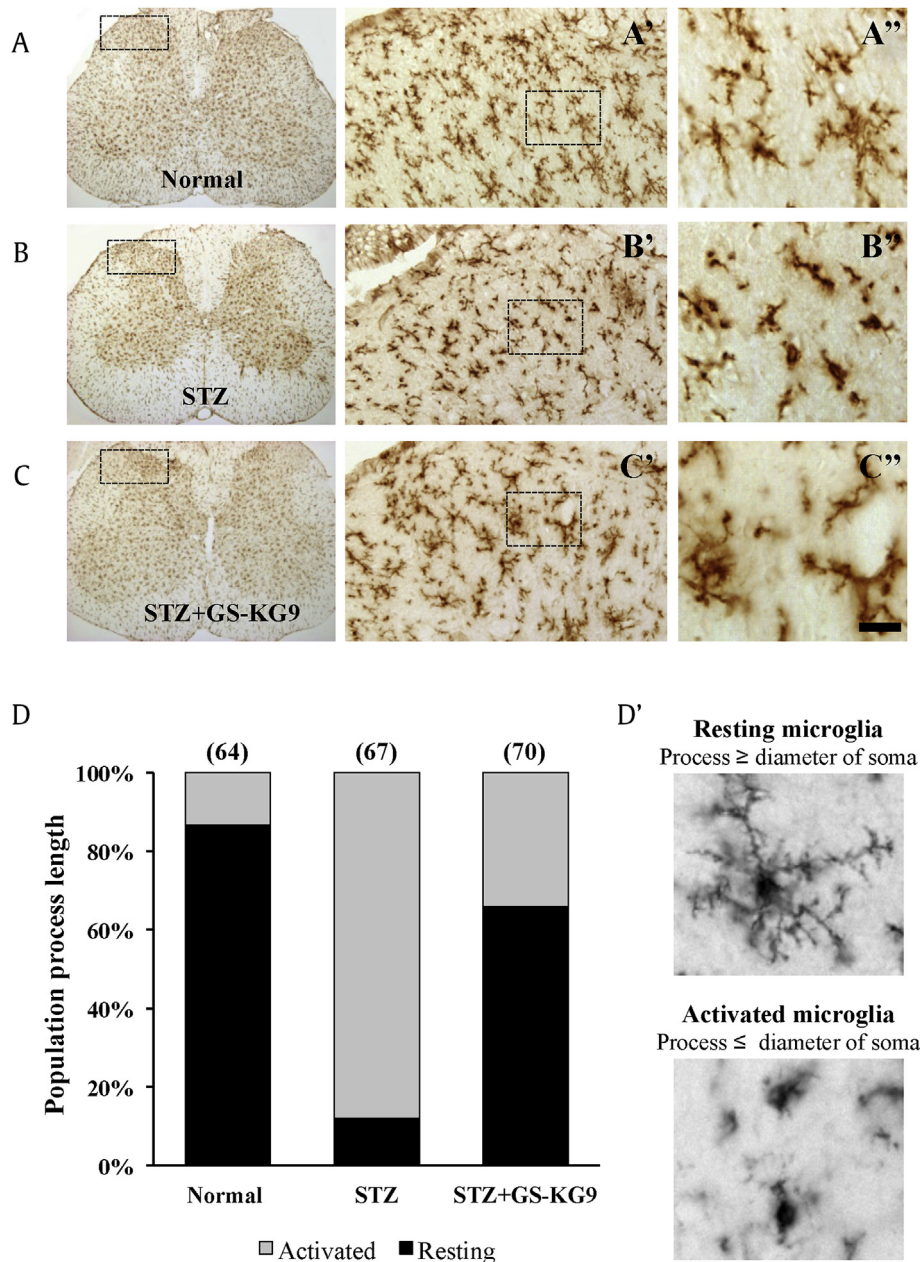
Fig. 4. GS-KG9 inhibits microglial activation in the lumbar (L4–L5) spinal cord. At 28 d after GS-KG9 (300 mg/kg) treatment, L4–L5 spinal tissues were prepared and immuno-stained with an OX-42 antibody. (A–C) Immunohistochemistry for OX-42 in the lumbar spinal cord. (A″–C″) High magnification of dotted boxes in the dorsal horn (A′–C′). Scale bar, 20μm. (D) Quantitative analyses show that GS-KG9 significantly reduced the proportion of activated microglia compared to the STZ control (n = 5 rats/group). Resting and activated microglia (D′) were classified and counted. Data are expressed as the mean ± standard deviation. STZ, streptozotocin.

hyperglycemic rats. However, STZ-induced microglial activation was significantly attenuated in the VPL of GS-KG9-treated rats. Densitometric analysis revealed that OX-42 immunoreactive intensity in GS-KG9-treated group (STZ + GS-KG9) was significantly lower than that in the vehicle control (STZ only; Fig. 6D). Thus, these data indicate that GS-KG9 inhibited microglia activation in the thalamic VPL nucleus in STZ-induced hyperglycemic rats.

4. Discussion

P. ginseng is one of the most popular herbal medicines used worldwide as a health-promoting food. The major ingredients associated with its various pharmacological activities are the gin-senosides. In addition to protopanaxadiol compounds, four

different malonyl ginsenosides (m-Rb1, m-Rb2, m-Rc, and m-Rd) were found in air-dried and ethanol extracted white ginseng, which is so-called GS-KG9. We had two reasons to examine whether GS-KG9 showed any suppressive activity on diabetic neuropathic pain. First, there are approximately 100 published papers about the antinociception of ginseng, but none has investigated the inhibitory effect of ginseng on diabetic neuropathic pain induced by STZ. Second, previous studies have focused on red ginseng, because structural changes in ginsenosides induced by steam process are thought to be concerned with the improved pharmacological activities of ginseng [25,26]. Among various types of commercial ginseng products, including fresh ginseng, white ginseng, and red ginseng, there are few studies on ginseng extract containing malonyl ginsenosides; probably due to difficulty in analyzing by
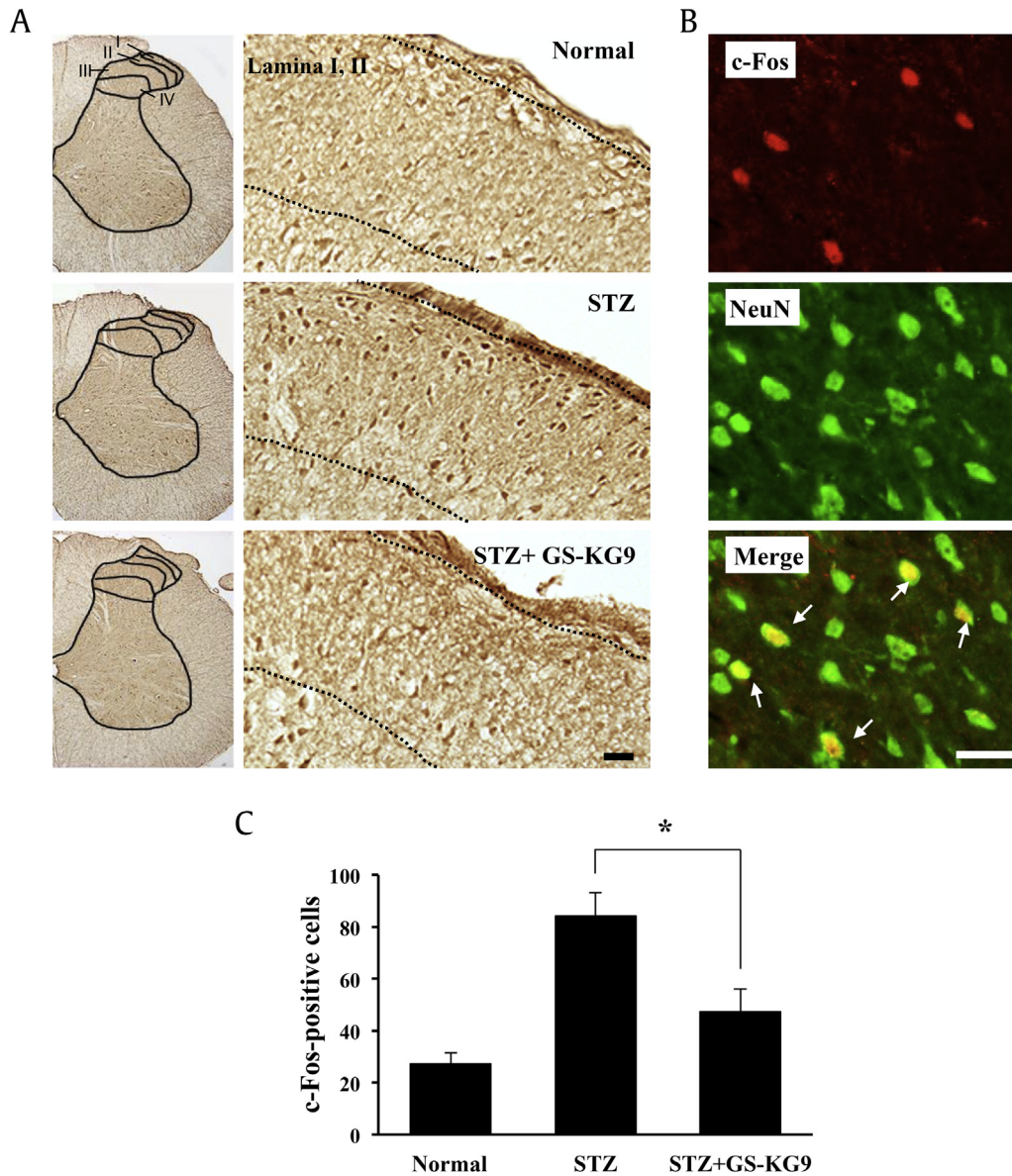
Fig. 5. GS-KG9 inhibits the expression of c-Fos in spinal cord dorsal horn in STZ-induced hyperglycemic rats. At 28 d after GS-KG9 (300 mg/kg) administration, lumbar (L4−L5) spinal tissues were prepared and immunostained with a c-Fos antibody. (A) Immunohistochemistry of c-Fos. Right panels are high magnification images (200×). Dotted line indicates c-Fos-positive cells in superficial layer (lamina I, II) of dorsal horn following STZ treatment. (B) Double labeling showed that c-Fos immunoreactivity was colocalized in NeuN-positive neurons (arrows). Scale bars, 30μm. (C) Quantitative analysis of c-Fos-positive cells in lamina I, II ($n = 5$ rats/group). Data are expressed as the mean ± standard deviation. *$p < 0.05$ versus STZ control. STZ, streptozotocin.

HPLC. We believe that consuming air-dried fresh ginseng-containing ginsenosides with malonyl moiety are a more natural way than heat- or steam-dried ginseng products.

Neuropathic pain is a functional disorder or pathological changes in a nerve and characterized by increased sensitivity to mechanical and thermal stimuli [27]. Neuropathic pain is often present and difficult to treat in diabetes mellitus [28,29]. Oxidative stress due to hyperglycemia is a primary contributor for the nerve malfunction depicted as symmetrical polyneuropathy [30]. Here, we examined the effects of GS-KG9 on neuropathic pain induced by STZ in mechanical and thermal pain behavior, and also figured out whether GS-KG9 exhibits any inhibitory activities upon microglial activation within the spinothalamic tract ascending from the spinal cord dorsal horn to ventral posterolateral nucleus of the thalamus.

The mechanisms underlying the development and maintenance of diabetic neuropathic pain include multiple biochemical and anatomical alterations in the peripheral and central nervous systems. Hyperglycemia is a causative requisite for hypersensitive pain associated with diabetes [31]. Hyperglycemia results in changes in the local microenvironment in the spinal cord, leading to microglial activation. For example, treatment of microglial cells with high glucose concentrations causes the release of interleukin-8 and reactive oxygen species, protein kinase C phosphorylation, and thereby activates the NF-κB signaling pathway. Parallel to cell studies, reactive oxygen species, protein kinase C, and NF-κB signaling pathway are induced or activated by hyperglycemia in diabetes [32,33]. Taken together, these reports suggest that hyperglycemia is responsible for microglial activation in diabetic neuropathic pain. It has also been reported that activated microglia
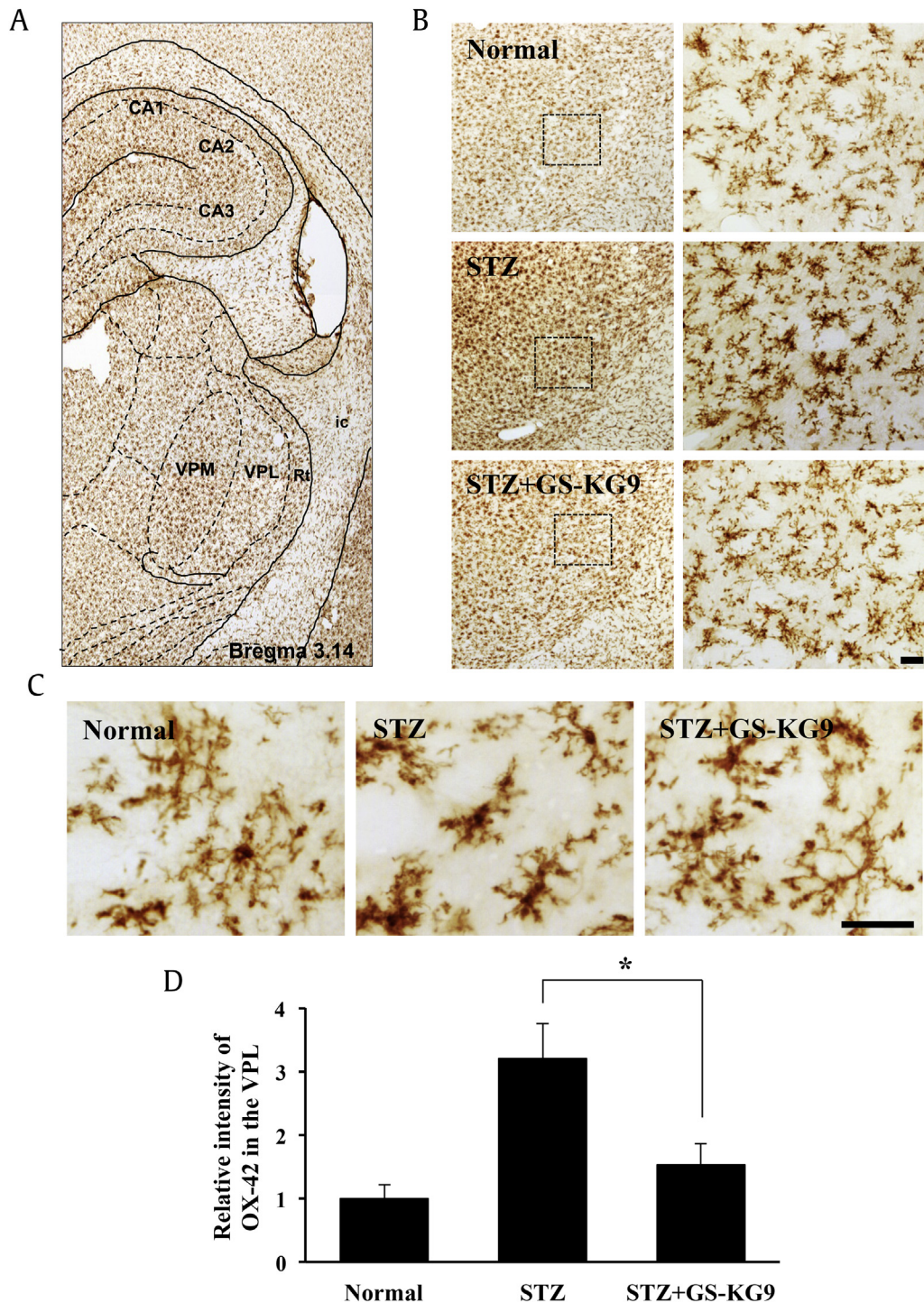
Fig. 6. GS-KG9 inhibits microglial activation in the thalamic VPL. At 28 d after GS-KG9 (300 mg/kg) administration, brain tissues containing VPL region were prepared and immunostained with an OX-42 antibody. (A, B) Immunohistochemistry of OX-42 in the VPL region. (B, right panels) and (C) are high magnification images. Scale bars, 50μm. (D) Densitometric analysis reveals the relative intensity of OX-42 immunoreactivity in the VPL ($n = 5$ rats/group). Data are expressed as the mean $\pm$ standard deviation. *$p < 0.05$ versus STZ control. STZ, streptozotocin; VPL, ventral posterolateral; VPM, ventral posteromedial.

and astrocytes in the spinal cord dorsal horn lead to the development of chronic pain by releasing proinflammatory cytokines [15,34]. Our data show that GS-KG9 lowers the blood glucose level and inhibits microglial activation in L4–L5 spinal cord in STZ-induced hyperglycemic rats (Figs. 2A and 4), which means that the analgesic effect of GS-KG9 might be mediated by inhibiting microglia activation through reducing blood glucose level.

Diabetes is also characterized by chronic inflammation partly due to hyperglycemia and insulin resistance, and activation of inflammatory cascades plays a pivotal role in the development and persistence of neuropathic pain [35]. Tsuda et al. [36] and Wodarshi et al. [11] independently reported that microglia play a role in the induction of diabetic neuropathic pain. Pabreja et al. [37] also showed that minocycline attenuates the development of diabetic

neuropathic pain by inhibiting inflammation and oxidative stress. Recently, we reported that increase in voltage-gated sodium channel current elicits microglial activation and followed by inflammatory responses *in vitro* and *in vivo* [38]. Furthermore, some studies have shown that Nav1.7 and 1.8 were overexpressed and the transient sodium current was increased significantly in small dorsal root ganglion neurons in STZ-induced hyperglycemic rats [39,40]. Thus, it will be interesting to examine whether GS-KG9 inhibits the expression of sodium channels in dorsal root ganglion neurons or decreases voltage-gated sodium current in microglia, and which components of GS-KG9 account for these pharmacological effects. Perhaps a future study will explain the underlying mechanism of the analgesic effect of GS-KG9 in diabetic neuropathic pain.

c-Fos is overexpressed in spinal cord dorsal horn neurons activated by nociceptive-related stimuli, and involved in neuropathic pain after peripheral and central nerve injury [41–43]. Some studies have also demonstrated that electrophysiological recording in hyperglycemic rats shows higher activity of spinal dorsal horn neurons [21,44]. c-Fos-positive cells in lamina I and II of dorsal horns were increased in STZ-induced hyperglycemic rats when compared to those in normal rats. However, GS-KG9 significantly reduced c-Fos-positive cells in the L4–L5 dorsal horn neurons as compared to those in STZ-treated control rats, suggesting that GS-KG9 inhibits hyperexcitability of spinal cord dorsal horn neurons in STZ-induced hyperglycemic rats, and thereby attenuates diabetic neuropathic pain.

Supraspinal regions as well as the spinal cord are known to be involved in neuropathic pain. The VPL nucleus of the thalamus is one of the most important areas in the central nervous system and plays a crucial role in pain signaling. LeBlanc et al. [45] demonstrated that minocycline injection into the VPL of the thalamus inhibits thermal hyperalgesia in peripheral-nerve-injury-induced neuropathy by inhibiting microglial activation. In our study, microglial activation in the VPL of the thalamus was inhibited by GS-KG9 in STZ-induced hyperglycemic rats as compared to that in STZ controls. Recent reports show that Compound K and ginsenoside Rb1 metabolite exhibit neuroprotective effects by inhibiting microglial activation after experimental stroke [46,47]. Jang et al. [6] also showed that ginsenoside Rb1 attenuates acute inflammatory pain by inhibiting neuronal ERK phosphorylation via regulation of the Nrf2 and NF-κB pathways. Thus, based on our and previous reports, the analgesic effect of GS-KG9 in STZ-induced diabetic neuropathic pain might be mediated by inhibiting microglial activation in the VPL of the thalamus as well as L4–L5 spinal cord, although the effects of GS-KG9 on ERK and NF-κB activation were not examined in this study.

The present study demonstrated that GS-KG9 inhibited hyperglycemia and thereby alleviated the allodynia and hyperalgesia in STZ-induced hyperglycemic rats. Furthermore, the analgesic effect of GS-KG9 might be mediated by inhibiting microglial activation in the spinal cord and VPL of the thalamus. Taken together, our data suggest that GS-KG9 could be a health food that can be used for diabetic neuropathic pain.

Conflicts of interest

All contributing authors declare no conflicts of interest.

Acknowledgments

References

[1] Leinonen A, Hiilesmaa V, Andersen H, Teramo K, Kaaja R. Diurnal blood glucose profiles in women with gestational diabetes with or without hypertension. Diabet Med 2004;21:1181–4.

[2] Martins JO, Wittlin BM, Anger DB, Martins DO, Sannomiya P, Jancar S. Early phase of allergic airway inflammation in diabetic rats: role of insulin on the signaling pathways and mediators. Cell Physiol Biochem 2010;26:739–48.

[3] Xu JT, Xin WJ, Zang Y, Wu CY, Liu XG. The role of tumor necrosis factor-alpha in the neuropathic pain induced by lumbar 5 ventral root transection in rat. Pain 2006;123:306–21.

[4] Sommer C, Kress M. Recent findings on how proinflammatory cytokines cause pain: peripheral mechanisms in inflammatory and neuropathic hyperalgesia. Neurosci Lett 2004;361:184–7.

[5] Park JS, Park EM, Kim DH, Jung K, Jung JS, Lee EJ, Hyun JW, Kang JL, Kim HS. Anti-inflammatory mechanism of ginseng saponins in activated microglia. J Neuroimmunol 2009;209:40–9.

[6] Jang M, Lee MJ, Choi JH, Kim EJ, Nah SY, Kim HJ, Lee S, Lee SW, Kim YO, Cho IH. Ginsenoside Rb1 attenuates acute inflammatory nociception by inhibition of neuronal ERK phosphorylation by regulation of the Nrf2 and NF-κB pathways. J Pain 2016;17:282–97.

[7] Chaplan SR, Bach FW, Pogrel JW, Chung JM, Yaksh TL. Quantitative assessment of tactile allodynia in the rat paw. J Neurosci Methods 1994;53:55–63.

[8] Hargreaves K, Dubner R, Brown F, Flores C, Joris J. A new and sensitive method for measuring thermal nociception in cutaneous hyperalgesia. Pain 1994;32:77–88.

[9] Yune TY, Lee JY, Jung GY, Kim SJ, Jiang MH, Kim YC, Oh YJ, Markelonis GJ, Oh TH. Minocycline alleviates death of oligodendrocytes by inhibiting pro-nerve growth factor production in microglia after spinal cord injury. J Neurosci 2007;27:7751–61.

[10] Hains BC, Waxman SG. Activated microglia contribute to the maintenance of chronic pain after spinal cord injury. J Neurosci 2006;26:4308–17.

[11] Wodarski R, Clark AK, Grist J, Marchand F, Malcangio M. Gabapentin reverses microglial activation in the spinal cord of streptozotocin-induced diabetic rats. Eur J Pain 2009;13:807–11.

[12] Toth CC, Jedrzejewski NM, Ellis CL, Frey 2nd WH. Cannabinoid-mediated modulation of neuropathic pain and microglial accumulation in a model of murine type I diabetic peripheral neuropathic pain. Mol Pain 2010;17:6–16.

[13] Suzuki N, Hasegawa-Moriyama M, Takahashi Y, Kamikubo Y, Sakurai T, Inada E. Lidocaine attenuates the development of diabetic-induced tactile allodynia by inhibiting microglial activation. Anesth Analg 2011;113:941–6.

[14] Morgado C, Pereira-Terra P, Cruz CD, Tavares I. Minocycline completely reverses mechanical hyperalgesia in diabetic rats through microglia-induced changes in the expression of the potassium chloride co-transporter 2 (KCC2) at the spinal cord. Diabetes Obes Metab 2011;13:150–9.

[15] Zychowska M, Rojewska E, Kreiner G, Nalepa I, Przewlocka B, Mika J. Minocycline influences the anti-inflammatory interleukins and enhances the effectiveness of morphine under mice diabetic neuropathy. J Neuroimmunol 2013;262:35–45.

[16] Cheng KI, Wang HC, Chuang YT, Chou CW, Tu HP, Yu YC, Chang LL, Lai CS. Persistent mechanical allodynia positively correlates with an increase in activated microglia and increased P-p38 mitogen-activated protein kinase activation in streptozotocin-induced diabetic rats. Eur J Pain 2014;18:162–73.

[17] Silva M, Amorim D, Almeida A, Tavares I, Pinto-Ribeiro F, Morgado C. Pro-nociceptive changes in the activity of rostroventromedial medulla (RVM) pain modulatory cells in the streptozotocin-diabetic rat. Brain Res Bull 2013;96:39–44.

[18] Schreiber AK, Nones CF, Reis RC, Chichorro JG, Cunha JM. Diabetic neuropathic pain: physiopathology and treatment. World J Diabetes 2015;6:432–44.

[19] Naderi A, Asgari AR, Zahed R, Ghanbari A, Samandari R, Jorjani M. Estradiol attenuates spinal cord injury-related central pain by decreasing glutamate levels in thalamic VPL nucleus in male rats. Metab Brain Dis 2014;29:763–70.

[20] Chen X, Levine JD. Hyper-responsivity in a subset of C-fiber nociceptors in a model of painful diabetic neuropathy in the rat. Neuroscience 2001;102:185–92.

[21] Chen SR, Pan HL. Hypersensitivity of spinothalamic tract neurons associated with diabetic neuropathic pain in rats. J Neurophysiol 2002;87:2726–33.

[22] Huber JD, Campos CR, Mark KS, Davis TP. Alterations in blood-brain barrier ICAM-1 expression and brain microglial activation after lambda-carrageenan-induced inflammatory pain. Am J Physiol Heart Circ Physiol 2006;290:H732–40.

[23] Zhao P, Waxman SG, Hains BC. Modulation of thalamic nociceptive processing after spinal cord injury through remote activation of thalamic microglia by cysteine chemokine ligand 21. J Neurosci 2007;27:8893–902.

[24] Wasserman JK, Koeberle PD. Development and characterization of a hemor-rhagic rat model of central post-stroke pain. Neuroscience 2009;161:173–83.

[25] Kim WY, Kim JM, Han SB, Lee SK, Kim ND, Park MK, Kim CK, Park JH. Steaming of ginseng at high temperature enhances biological activity. J Nat Prod 2000;63:1702–4.

[26] Sun S, Qi LW, Du GJ, Mehendale SR, Wang CZ, Yuan CS. Red notoginseng: higher ginsenoside content and stronger anticancer potential than Asian and American ginseng. Food Chem 2011;125:1299−305.

[27] Rasmussen PV, Sindrup SH, Jensen TS, Bach FW. Symptoms and signs in patients with suspected neuropathic pain. Pain 2004;110:461−9.

[28] Jolivalt CG, Lee CA, Ramos KM, Calcutt NA. Allodynia and hyperalgesia in diabetic rats are mediated by GABA and depletion of spinal potassium-chloride cotransporters. Pain 2008;140:48−57.

[29] Said G. Diabetic neuropathy − a review. Nat Clin Pract Neurol 2007;3:331−40.

[30] Calcutt NA. Potential mechanisms of neuropathic pain in diabetes. Int Rev Neurobiol 2002;50:205−28.

[31] Courteix C, Bardin M, Massol J, Fialip J, Lavarenne J, Eschalier A. Daily insulin treatment relieves long-term hyperalgesia in streptozotocin diabetic rats. Neuroreport 1996;7:1922−4.

[32] Obrosova IG. Diabetic painful and insensate neuropathy: pathogenesis and potential treatments. Neurotherapeutics 2009;6:638−47.

[33] Obrosova IG. Diabetes and the peripheral nerve. Biochim Biophys Acta 2009;1792:931−40.

[34] Austin PJ, Moalem-Taylor G. The neuro-immune balance in neuropathic pain: involvement of inflammatory immune cells, immune-like glial cells and cytokines. J Neuroimmunol 2010;229:26−50.

[35] Galloway C, Chattopadhyay M. Increases in inflammatory mediators in DRG implicate in the pathogenesis of painful neuropathy in Type 2 diabetes. Cytokine 2013;63:1−5.

[36] Tsuda M, Ueno H, Kataoka A, Tozaki-Saitoh H, Inoue K. Activation of dorsal horn microglia contributes to diabetes-induced tactile allodynia via extracellular signal-regulated protein kinase signaling. Glia 2008;56:378−86.

[37] Pabreja K, Dua K, Sharma S, Padi SS, Kulkarni SK. Minocycline attenuates the development of diabetic neuropathic pain: possible anti-inflammatory and antioxidant mechanisms. Eur J Pharmacol 2011;661:15−21.

[38] Jung GY, Lee JY, Rhim H, Oh TH, Yune TY. An increase in voltage-gated sodium channel current elicits microglial activation followed inflammatory responses *in vitro* and *in vivo* after spinal cord injury. Glia 2013;61:1807−21.

[39] Hong S, Morrow TJ, Paulson PE, Isom LL, Wiley JW. Early painful diabetic neuropathy is associated with differential changes in tetrodotoxin-sensitive and -resistant sodium channels in dorsal root ganglion neurons in the rat. J Biol Chem 2004;279:29341−50.

[40] Sun YM, Su Y, Li J, Tian Y, Wang LF. Role of the Na(+)/H(+) exchanger on the development of diabetes mellitus and its chronic complications. Biochem Biophys Res Commun 2012;427:229−31.

[41] Kawahara H, Sakamoto A, Takeda S, Onodera H, Imaki J, Ogawa R. A prostaglandin E2 receptor subtype EP1 receptor antagonist (ONO-8711) reduces hyperalgesia, allodynia, and c-fos gene expression in rats with chronic nerve constriction. Anesth Analg 2001;93:1012−7.

[42] Hossaini M, Duraku LS, Kohli SK, Jongen JL, Holstege JC. Spinal distribution of c-Fos activated neurons expressing enkephalin in acute and chronic pain models. Brain Res 2014;1543:83−92.

[43] Siddall PJ, Xu CL, Floyd N, Keay KA. C-fos expression in the spinal cord of rats exhibiting allodynia following contusive spinal cord injury. Brain Res 1999;851:281−6.

[44] Pertovaara A, Wei H, Kalmari J, Ruotsalainen M. Pain behavior and response properties of spinal dorsal horn neurons following experimental diabetic neuropathy in the rat: modulation by nitecapone, a COMT inhibitor with antioxidant properties. Exp Neurol 2001;167:425−34.

[45] LeBlanc BW, Zerah ML, Kadasi LM, Chai N, Saab CY. Minocycline injection in the ventral posterolateral thalamus reverses microglial reactivity and thermal hyperalgesia secondary to sciatic neuropathy. Neurosci Lett 2011;498:138−42.

[46] Bae MY, Cho JH, Choi IS, Park HM, Lee MG, Kim DH, Jang IS. Compound K, a metabolite of ginsenosides, facilitates spontaneous GABA release onto CA3 pyramidal neurons. J Neurochem 2010;114:1085−96.

[47] Park JS, Shin JA, Jung JS, Hyun JW, Van Le TK, Kim DH, Park EM, Kim HS. Anti-inflammatory mechanism of compound K in activated microglia and its neuroprotective effect on experimental stroke in mice. J Pharmacol Exp Ther 2012;341:59−67.